PERGAMON

Acta mater. Vol. 47, No. 9, pp. 2717–2726, 1999

Printed in Great Britain
PII: S1359-6454(99)00140-8
1359-6454/99 $20.00 + 0.00

ELECTROPHORETIC DEPOSITION FORMING OF POROUS ALUMINA MEMBRANES

C.-Y. CHEN[1], S.-Y. CHEN[1] and D.-M. LIU[2]†

[1]Department Materials Science and Engineering, National Chao-Tung University, Ta-Hsueh Rd, Hsinchu, Taiwan 300 and [2]Department of Materials Science and Engineering, University of Pennsylvania, 3231 Walnut Street, Philadelphia, PA 19104, U.S.A.

(Received 19 November 1998; accepted 14 April 1999)

Abstract—An electrophoretic deposition (EPD) technique is used to prepare porous alumina membranes. The deposition kinetics which are conventionally derived based on a mass conservation law have been modified in terms of the thickness of the deposited layer. This modification allows the porosity evolution of the membrane to be predicted under a variety of EPD processes. A transition in deposition from linear to parabolic kinetics is observed which has been further verified by a subsequent microstructure examination. The deposited layers are increasingly uniform and dense in structure with increasing deposition time over the parabolic kinetic regime; whilst a more porous packing is observed during the initial deposition time period, corresponding to the linear kinetic regime. The microstructural evolution of the EPD membranes appears to agree well with the porosity equations derived based on an analytical combination of both experimentally-derived formula and the corresponding kinetic model. © *1999 Acta Metallurgica Inc. Published by Elsevier Science Ltd. All rights reserved.*

Keywords: Powder consolidation; Sintering; Powder processing; Scanning electron microscopy (SEM); Ceramics; Structural; Microstructure

1. INTRODUCTION

Electrophoretic deposition (EPD) is an old but effective technique to fabricate thin or thick ceramic films upon a variety of conductive substrates [1–6]. In the EPD process, the electrodes (or substrates) are immersed into a ceramic suspension within which the ceramic particles are charged and well dispersed. Whilst subjected to a d.c. voltage, the charged particles move towards the electrode surface (hereafter named the target surface) of opposite charge. The particles impact onto the surface of the electrode and form layers of different thicknesses. The deposited layer is then fired at high temperatures, to obtain, as observed in most practical applications, dense thick ceramic films or thin ceramic sheets (e.g. 1–5 μm thickness) [4] and their laminate structure [7, 8]. However, since the pores can be evolved in a controlled manner either by a chemical means [9, 10], e.g. using a sol–gel route, or by the formation of interstices and/or voids in a particle packing structure, e.g. using a conventional casting route from powder suspensions, it may be interesting to prepare a porous membrane by means of EPD. This is the focus of this investigation. Available reports on the fabrication of porous membranes through the EPD route are not widespread in the literature [11, 12].

In this investigation, an alumina powder suspension is prepared as a model suspension for EPD membrane fabrication onto a porous stainless-steel substrate. A narrow pore size distribution together with a suitable pore volume fraction, with mostly an interconnected pore structure, are most desirable for porous membranes. The former requirement ensures a service quality of the membrane while the latter allows sufficient permeability during service. To achieve these, better particle packing from a well-dispersed suspension appears essential. This is because poor particle packing, e.g. due to particle agglomeration, would cause inhomogeneities such as a broader pore distribution or a multi-model pore distribution in the final membrane structure, resulting in a poor service performance and reliability as well. Therefore, the influence of suspension pH, powder dispersion, and particularly the EPD parameter, e.g. applied d.c. voltage, on the microstructure of the EPD membranes and the deposition kinetics is the main concern of this investigation.

2. EXPERIMENTAL PROCEDURES

The suspensions were prepared by mixing alumina powder (AKP-50, Japan) having an average particle size of 0.2 μm with ethanol (95% purity and 5% water, Aldrich, U.S.A.) in a ball miller for 24 h. The grinding media were high-purity alumina balls. The pH value of the suspensions was adjusted over a

†To whom all correspondence should be addressed.

range from ~2.2 to ~11 using HCl or HN_4OH. The particles were subsequently characterized using zeta potentiometry (Brovkaven, Model Zetaplus) to determine the isoelectric point (IEP) and particle size analysis (Microtrac-UPA 150) to study the dispersion of the particles in the suspensions. The stability of the suspensions was judged qualitatively after 24 h sedimentation by visual examination.

The suspensions exhibiting the best dispersion characteristics were used as model suspensions for EPD membrane preparation. The EPD process was performed by immersing two parallel stainless-steel substrates (as electrodes) with a separation of 3 cm into the selected suspensions (containing 100 ml of ethanol and 9 g of alumina powder) and up to a constant voltage of $E = 100$ V was applied between the two electrodes. The surface area immersed into the suspensions for EPD is $2 \times 2.5\ cm^2$ for the target electrode. The thickness of the deposited layer was measured using scanning electron microscopy (Cambridge Instrument, S360) and characterized as a function of deposition time (t) for kinetic investigation. The thickness of the deposited layer is determined by averaging two–three samples prepared from different batches of suspensions under identical preparation conditions. The pore size as well as the porosity of the EPD membranes were examined by using mercury porosimetry (AutoPore 9200) after the membranes were fired at a temperature of 1150°C for 2 h in a reduced atmosphere.

3. RESULTS AND DISCUSSION

3.1. Particle dispersion and suspension stability

The zeta potential of the particles was measured and showed an isoelectric point (IEP) at pH 9 (Fig. 1), consistent with values reported in the literature. The stability of the as-prepared suspensions of different pH values was judged by placing the suspension into a glass tube for observation over a period of 24 h. Over the pH range of study, we found that lower pH values resulted in more stable suspensions, and more specifically, no appreciable phase separation was observed at a solution pH of ~2.2 over the time span of the test. However, under higher pH, e.g. at pH of ~11, the suspensions were less stable. This seems to be explainable based on a charging mechanism recently proposed by Wang *et al.* [13] on the alumina surface, which has

$$AlOH_2^+ \Leftarrow^{H^+} AlOH \Longrightarrow^{OH^-} AlO^- + H_2O.$$

Under basic conditions such as pH ~11, AlOH tends to form AlO^-; however, the presence of water is prone to bring the above reaction towards the formation of $AlOH_2^+$, rather than the formation of AlO^-, resulting in an absolute value of the zeta potential greater at pH ~2 than at pH ~11. This is therefore the major reason of current experimental observation where the suspensions were less stable at higher pH than at lower pH conditions.

The stable suspension at pH ~2.2 suggests that the particles are sufficiently dispersed in the liquid medium. A subsequent particle size analysis of the suspension showed a unimodel distribution with an average particle size of about 0.3 μm, consistent with the size range of 0.1–0.3 μm reported by the supplier. Therefore, suspensions with a pH value of 2.2 were selected as the model suspension for EDP membrane preparation.

3.2. Electrophoretic deposition

3.2.1. Effect of suspension pH on deposition: a qualitative observation. Table 1 shows visual observations on membranes deposited under $E = 100$ V for 60 s. Clearly, increasing the pH of the solution leads to poor deposition, resulting in an uneven

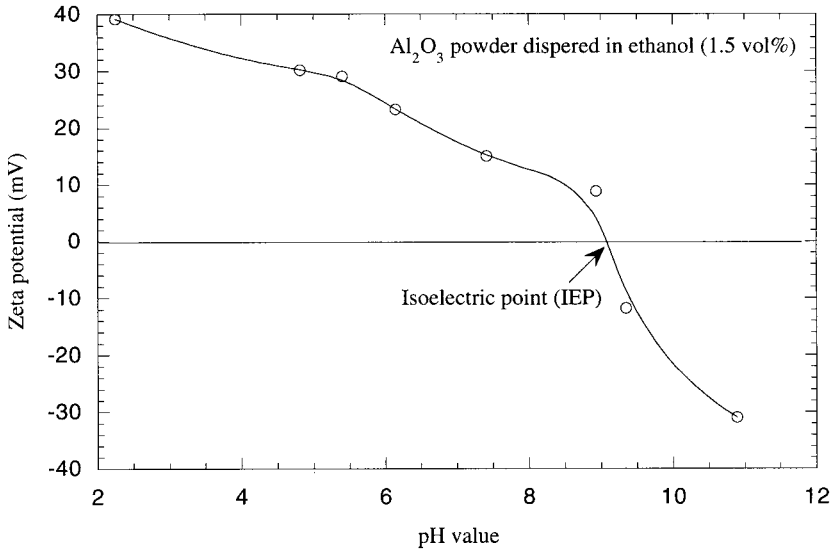

Fig. 1. The zeta potential of the Al_2O_3 powder in ethanol.

Table 1. Visual observations on EPD membranes deposited under 100 V d.c. for 60 s with suspensions of different pH values

Suspension pH	Membrane conditions
2.25	uniform thickness, good adhesion to substrate, no cracking after drying
4.37	good adhesion but cracking after drying
5.60	fair adhesion and peeling after drying
9.36	poor adhesion, non-uniform thickness, peeling after drying
10.05	no adhesion to substrate
11.12	no adhesion to substrate

membrane surface and cracking after drying. Furthermore, little or a negligible amount of deposition can be visually seen at pH greater than ~9, a solution condition which is supposed to deposit the negatively-charged particles onto the anode surface. One possibe reason may arise from the lower values of zeta potential which correspond to a lower rate of particle mobility under basic conditions, especially in such a short time period of deposition. Furthermore, under those basic conditions, i.e. pH > 9.0, the suspensions are unstable and the particles are strongly agglomerated, further weakening the deposition ability.

The best deposition can be achieved at pH 2.2, where the deposited layer is microstructurally homogeneous and no surface cracking is observed after ambient drying. The adhesion between the substrate and deposited layer appears to be good.

3.2.2. Membrane thickness. The thickness (h) of the deposited membranes was measured as a function of deposition time and applied d.c. voltage, as shown in Fig. 2. Obviously, an increase in the applied d.c. voltage leads to an increased thickness, up to a maximum for this experiment of 200 μm at $E = 100$ V for 360 s. The time (t)–thickness (h) relations are likely to follow a similar function irrespective of the applied d.c. voltages over the time span of deposition. Therefore, a better understanding of the time–thickness correlation, i.e. a kinetic relation, should be practically and technologically important in manipulation of the membrane structure for specific applications during its preparation. Conventionally, a mass conservation law is used to account for the deposition kinetics [14] and most analytical derivations have recognized the weight (w) of deposition as a linear function and the square root of deposition time, $t^{1/2}$, for sufficient time of deposition. This relationship is linear with time (t) only at the very beginning of deposition [15, 16].

In this study we use the thickness (h) as the major parameter, instead of the weight, to model the deposition kinetics. According to a recent kinetic equation proposed by Zhang *et al*. [14] based on the mass conservation law, the deposited weight (w) can be expressed as an exponential function of t by

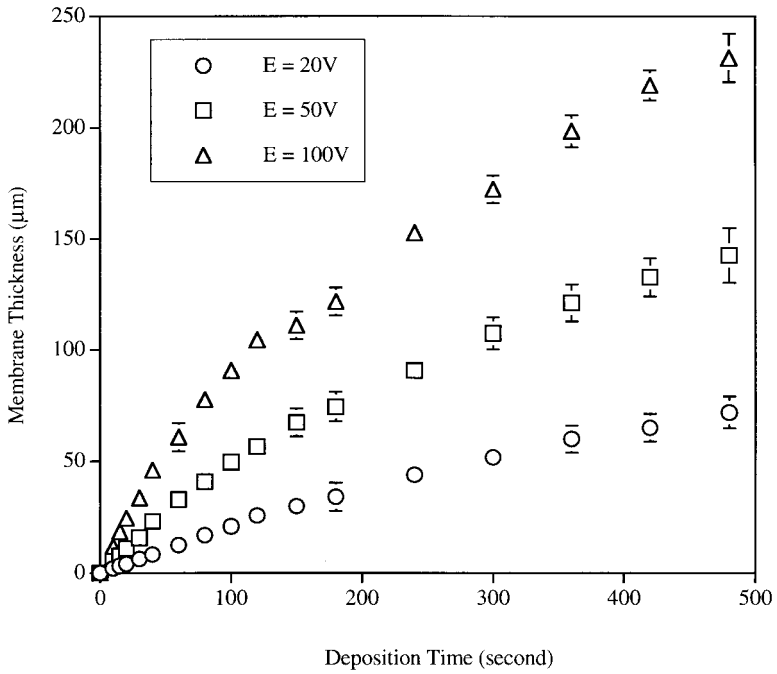

Fig. 2. Membrane thickness as a function of deposition time for different applied d.c. voltages.

$$\frac{dw}{dt} = w_0 k \exp(-kt) \quad (1)$$

where

$$k = \frac{A}{V}\frac{\varepsilon\xi}{4\pi\eta}(E - \Delta E)$$

w_0 is the initial solid weight in the suspension, A the surface area of the target electrode, V the slurry volume, ε the dielectric constant of the liquid, ξ the zeta potential of the particle in solvent, h the viscosity of the solvent, E the applied d.c. voltage and ΔE the voltage drop across the deposited layer.

For the case of a constant solid concentration, we can simplify equation (1) as

$$\frac{dw}{dt} = k' \exp(-kt). \quad (2)$$

When the time of deposition is relatively short, equation (2) can be simplified into the form

$$w = k't = w_0 kt \quad (3)$$

where a linear relation between w and t is expected. However, for a long deposition time period, equation (1) can be approximated to that suggested by Sussman and Ward [16]

$$w = (D^2 + Bt)^{1/2} - D \quad (4)$$

where D and B are constants and the deposited weight is essentially a linear function of $t^{1/2}$.

By choosing the thickness as the critical parameter, we presume that the total amount (corresponding to deposited weight) of particles deposited on the target surface, and those deposited on other electrode surfaces are negligibly small. In fact, the resulting experimental observation agrees with this assumption and this allows us to formulate the deposited weight as a function of thickness, h, as

$$w = Ah\rho(1 - P) \quad (5)$$

where A is the surface area of the target electrode required for the deposition, ρ the density of the particles, and P the porosity of the deposited layer and $1 - P$ is essentially the solid fraction of the particle packing structure. Substituting equation (5) into equation (2), we can thus have

$$\frac{dh}{dt} = \frac{k''}{1 - P}\exp(-kt) \quad (6)$$

where

$$k'' = \frac{k'}{A\rho} = \frac{w_0 k}{A\rho} = \frac{w_0}{V\rho}\frac{\varepsilon\xi}{4\pi\eta}(E - \Delta E)$$

having the unit of velocity, cm/s.

By analogy, for short deposition times, the deposited thickness should be linearly proportional to t, similar to equation (3) and have the form of

$$h = \frac{k''}{1 - P}t. \quad (7)$$

For prolonged deposition time, h is proportional to $t^{1/2}$. One interesting finding in equation (6) or equation (7) is the incorporation of porosity (P) which, in our opinion, should be critical especially when a porous membrane is to be prepared. However, whether P (or $1 - P$) should be treated as a constant is not realized and a later microstructural observation suggests that the porosity P shoud be varied as the deposited layer is growing over some critical thickness.

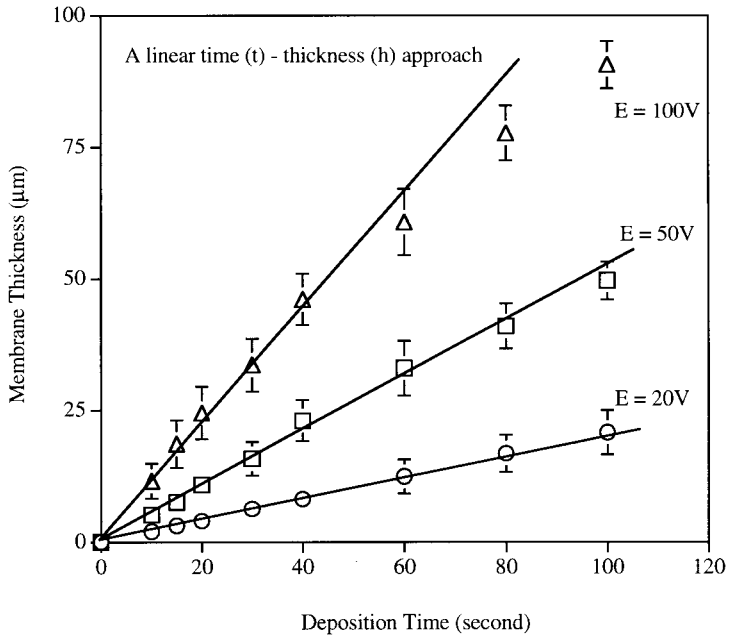

Fig. 3. A linear time (t)–thickness (h) approach for short time period of deposition.

To further elucidate the t–h relationship, we first focused on the thickness of the deposited layer at short time period and the results are shown in Fig. 3 for different d.c. voltages. A linear t–h function can generally be observed (as shown by the solid lines). This linearity appears to be particularly pronounced in the cases of lower d.c. voltages, e.g. $E<50$ V, and the fitting appears best at the lowest voltage, 20 V. Such linear t–h kinetics are likely to remain over a certain time duration, depending on the voltage applied, for instance, at $E = 20$ V the t–h linearity sustains over $t > 100$ s and up to $t \sim 60$ s at $E = 50$ V and to ~30 s at $E = 100$ V. The corresponding thickness of the deposited layer is approximately in the range of 20–25 μm at 20 V, 30–35 μm at 50 V, and 35–40 μm at 100 V as observed experimentally. The layers greater than these critical thicknesses show a transition to weaker time-dependent kinetics (i.e. the layer thickness no longer follows the solid lines depicted in Fig. 3, falling below them). This kinetic transition is believed to result from a voltage drop across the deposited layer, resulting in a lower electrophoretic force for the deposition. Here, it may be worth mentioning that the time span on such a linear t–h kinetics can be evaluated in a quantitative manner, in comparison to those based only on a qualitative approach [14, 16]. In this investigation, we believe the deposition kinetics can be linearly related to t over some reasonable time period especially at lower applied voltages. This is due to a slower growth of the deposited layer at lower E, corresponding to a lower degree of voltage drop (Fig. 4).

The voltage drop across the deposited membrane was determined by recording the starting electric current (I_0) under a voltage E_0. When the membrane developed to a thickness h (at time t), the electric current declined to I_1 and at the mean time, the voltage was adjusted to a higher value E_1 resulting in an electric current identical to the starting current. The difference of $E_1 - E_0$ (ΔE) is then defined as the voltage drop. As shown in Fig. 4, the higher the d.c. voltage applied, the greater the extent of the resulting voltage drop. However, despite the different d.c. voltages applied, the transition seems to take place at an identical degree of voltage drop, i.e. $\Delta E/E = 2.5\%$. This suggests the linear t–h kinetics can only be sustained over a relatively small range of voltage drop across the deposited layer.

For prolonged depositions, the thickness exhibits a linear function of $t^{1/2}$ for all the applied d.c. voltages over the entire duration of the study, as illustrated in Fig. 5. Such a $t^{1/2}$ dependence substantiates weaker deposition kinetics compared with those observed in a short time period. In general, the slope in the $t^{1/2}$–h lines can often be treated as a rate constant which, according to equation (1), can be directly related to E provided the influence of ΔE on k is negligibly small. However, this would be a more reasonable approach for short deposition time where the voltage drop is relatively small. For long deposition time, for instance, in the case of a 300 s period at $E = 50$ V, a voltage drop as large as ~10% can be measured, which could cause considerable error, if neglected, in quantitative evaluation. Therefore, in order to have a better and more precise evaluation, attention will be first focused on the linear t–h regime.

3.2.3. Porosity evolution: a prediction from the kinetic model. The slope (S_1) of the lines in the linear t–h regime depicted in Fig. 3 should be identical to the value of k''/p described in equation (7), which

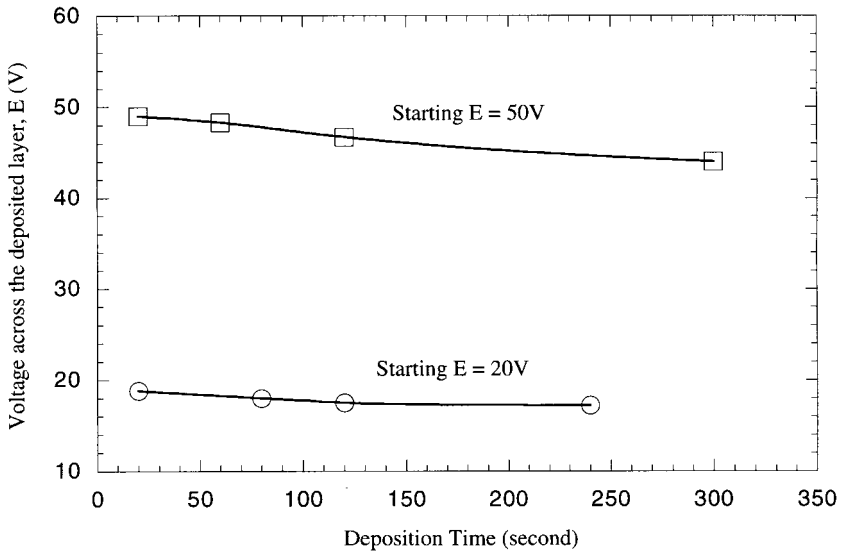

Fig. 4. The applied voltage change with increasing deposition time.

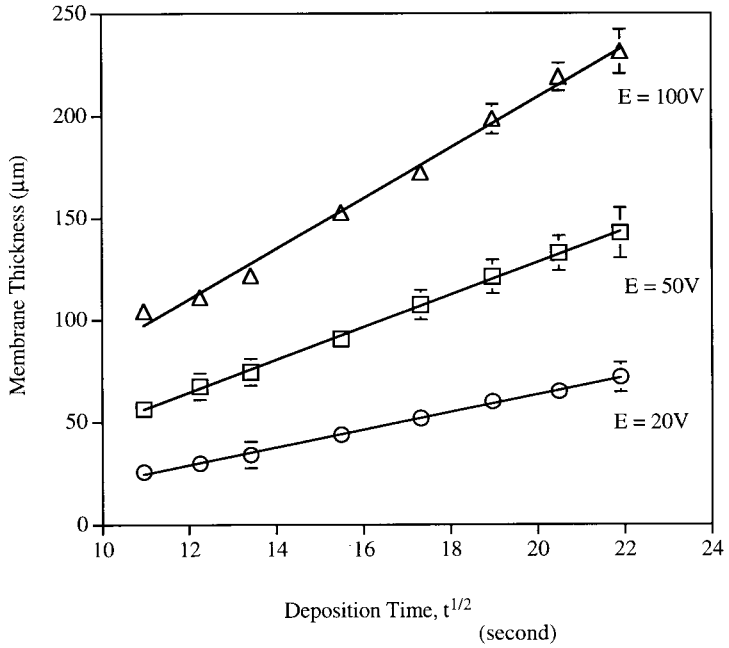

Fig. 5. A parabolic time (t)–thickness (h) approach for long time period of deposition.

yields

$$S_1 = \frac{k''}{1-P}. \tag{8}$$

For a given EPD condition, equation (8) suggests the porosity (or soild fraction, $f = 1 - P$) in the deposited structure should be a constant provided that the deposition is dominated by the linear t–h kinetics. The membrane porosity P can be calculated once both the slope (S_1) and k'' are known. This was done using the following values: $\varepsilon = 32.6$, $\xi = 3$ mV, $V = 100$ ml, $\rho = 3.98$ g/cm^3, $w_0 = 6.0$ g, and $\eta = 0.52$ mPa s, and the results are given in Table 2 for different d.c. voltages. It is interesting to note that the solid fraction f of the membrane can be reduced whilst applying an increased voltage. This is possible because the higher voltage gives a higher impact velocity of the particles onto the target surface. The time to deposit the particles may be too short for a better arrangement between particles to achieve an optimal packing structure. This finding suggests the porosity (as well as the pore size) of an EPD membrane can be easily manipulated via the variation of applied voltage. This would be important in the structural design of porous membranes, for example, a greater porosity in a membrane permits a more efficient permeability and this can be achieved via the EPD process with higher applied voltages.

Table 2. The solid fraction, $1 - P$, of the EPD membranes in the linear time (t)–thickness (h) kinetic regime under different applied d.c. voltages

Applied d.c. voltage, E	Solid fraction, $1 - P$ (volume fraction)
20	0.354
50	0.322
100	0.293

In this respect, it is interesting to realize, through a kinetic viewpoint, the evolution of porosity whilst the deposited layer is continuously growing in the $t^{1/2}$–h regimes. To elucidate this, the deposition rate ($\mathrm{d}h/\mathrm{d}t$) in equation (6) can be related to the differential form of the $t^{1/2}$–h lines by

$$\frac{S_2}{2}\frac{1}{t^{1/2}} = \frac{k''}{1-P}\exp(-kt). \tag{9}$$

After rearrangement, the porosity (or solid fraction) can be estimated by

$$1 - P = \frac{2k''}{S_2} t^{1/2} \exp(-kt). \tag{10}$$

Obviously, the porosity is unlikely to be a constant throughout the EPD processing over the $t^{1/2}$–h kinetic regime and this is substantially different from that observed in the linear kinetic regime, a constant P. The $(1 - P)$ can be enhanced with $t^{1/2}$ but decreased with $\exp(-kt)$. Here we use both voltages of 20 and 50 V as examples to demonstrate how the solid fraction $(1 - P)$ is changing with time, as calculated based on a set of values of $k = 0.363 \times 10^{-4}$/s, $S_2 = 4.2995 \times 10^{-4}$ cm/s, and $k'' = 0.0708 \times 10^{-4}$ cm/s for 20 V and $k = 0.906 \times 10^{-4}$/s, $S_2 = 7.9764 \times 10^{-4}$ cm/s, and $k'' = 0.177 \times 10^{-4}$ cm/s for 50 V. Figure 6 shows the resulting relationship where the solid fraction of the deposited layer increases with increasing deposition time in the $t^{1/2}$–h kinetic regime. A fraction

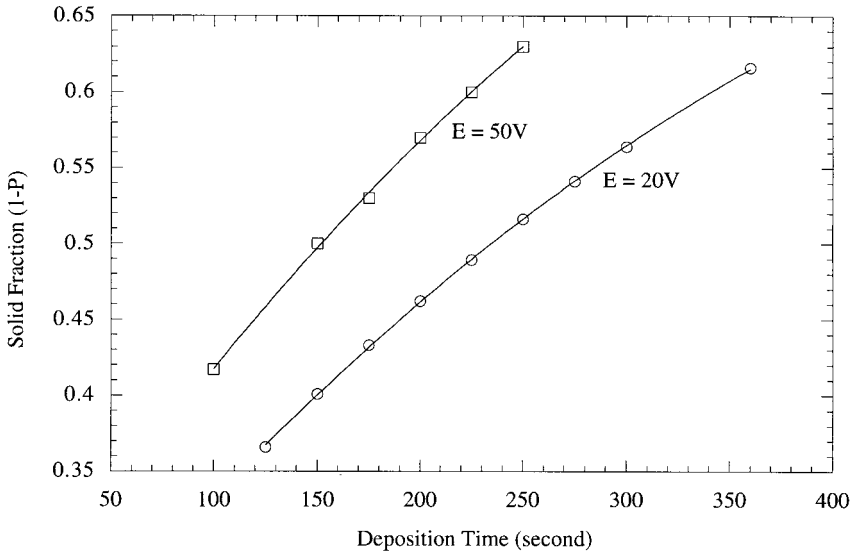

Fig. 6. The porosity as a function of deposition time under d.c. voltage of 20 and 50 V, based on equation (10).

of 0.366 after 125 s of deposition is estimated, which is slightly higher than the value in the linear kinetic regime having a constant $1 - P = 0.354$ (Table 2). This finding implies a porosity gradient can be developed within the membrane structure when the deposition is shifting from linear to parabolic kinetics. From a fabrication viewpoint, the EPD process can provide the resulting membranes with an *in situ* formation of porosity gradient, an advantage over the membranes modified by multilayer porous coatings for specific applications [9, 17–19].

However, we estimated the porosity at very short deposition time, e.g. < 10 s, if the parabolic kinetics still hold and the linear kinetics will only hold for $t \longrightarrow 0$ as generally assumed. The resulting calculation shows the membranes initially deposited can have a solid fraction as low as 3–5% of theoretical, corresponding to a porosity greater than 95%. These appear impossible because no such porous structure can be microscopically observed as evidenced in Fig. 7 where the membrane is deposited at $E = 50$ V for 5 s. Although indirectly, this seems to provide strong and more reasonable evidence for supporting the behavior of kinetic transition and corresponding models for microstructural evolution [equations (8) and (10)].

The point at which kinetic transition occurs can be determined by equalizing both equations (8) and (10) at a fraction value which is identical for both kinetic regimes. This results in

$$t^{1/2} \exp(-kt) = \frac{S_2}{2S_1}. \tag{11}$$

The t obtained in equation (11) is essentially the critical time (t_c) at the transition and it is obviously a function of applied voltage. By plotting the obtained t_c against E, Fig. 8 shows the resulting curve where the critical time is decreased exponentially with increasing voltage. The regime below the curve is dominated by linear kinetics, whilst above the curve, a parabolic-kinetic regime is dominant. The corresponding critical thickness of the deposited layers is also calculated and is depicted in parentheses, which is consistent in magnitude with the thickness obtained experimentally from Fig. 3.

3.2.4. Microstructure examination. To further elucidate the microstructural evolution of the deposited layer, particularly in those two kinetic regimes, we examined the microstructure of the deposited layer formed under $E = 50$ V at deposition times of 5 and 300 s as illustrated in Figs 9(a) and (b). The corresponding layer thicknesses are 6 μm (5 s) and 105 μm (300 s). Obviously, a better particle packing structure can be achieved at a longer deposition time (dominated by parabolic kinetics) than that of

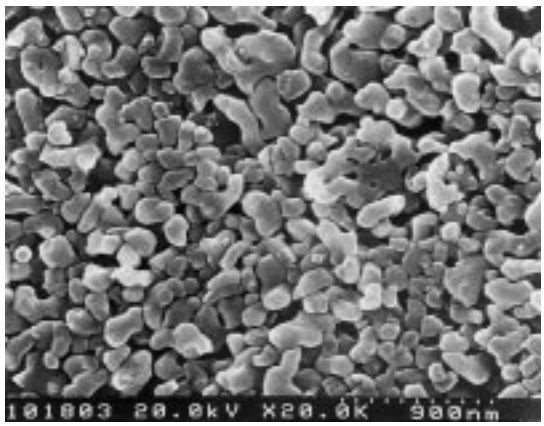

Fig. 7. Microstructure of the deposited layer prepared at $E = 50$ V for 5 s of deposition.

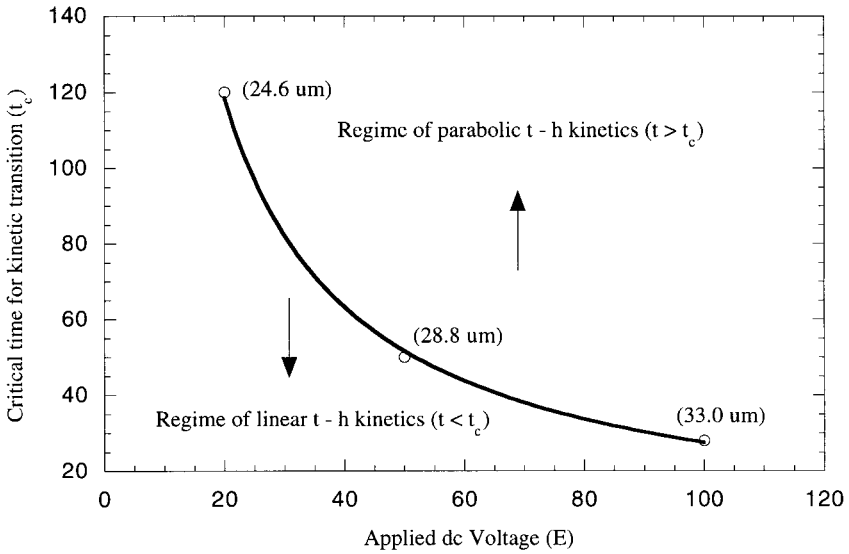

Fig. 8. The critical time of deposition as an exponential function of the applied voltage, the area below the curve suggests linear kinetics, whilst above the curve, a parabolic kinetic regime.

short deposition (dominated by linear kinetics). In the linear kinetic regime [Fig. 8(a)], the pores are much less uniform in size and distribution in comparison with those produced in the parabolic kinetic regime [Fig. 8(b)].

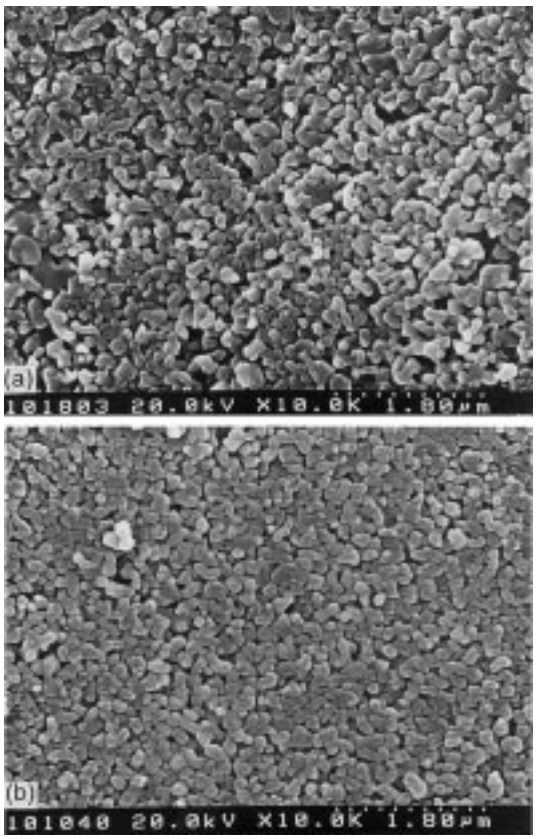

Fig. 9. Microstructural examination for the membranes deposited under $E = 50$ V for (a) 5 s and (b) 300 s, the pore structure becoming more uniform and smaller in size as well as distribution for longer time period of deposition.

Nevertheless, pores become much finer and more uniformly distributed as the deposition time proceeds over the parabolic regime. This observation qualitatively verifies the previous calculation of porosity evolution based on the parabolic kinetics defined in equation (10). This is an interesting discovery because it allows the microstructure evolution of the EPD membrane to be predicted and controlled through the use of kinetic. This, to our knowledge, may also be the first report on a quantitative and direct correlation between deposition kinetics and corresponding microstructural evolution in the preparation of porous membranes.

A pore size analysis for membranes prepared under $E = 100$ V for various time periods is shown in Fig. 10. Obviously, a smaller pore size and narrower pore distribution can be obtained after prolonged deposition time. The most frequent pore size is reduced by about 20%, shifting from 106.8 nm for 30 s to 85.7 nm for 300 s of deposition. This reduction in pore structure agrees with those observed in Fig. 9, which further provides a direct support for previous kinetic-based discussion. The pore distribution is essentially unimodal for membranes prepared over a sufficient time period of deposition, which, in turn, is suitable for microfiltration applications.

3.2.5. Microstructural evolution map in the EPD membranes. Based on the porosity model given in equations (8) and (10) and microstructural inspection (Fig. 9), it is conceivable that a microstructural evolution map appears to be effectively constructed. This is shown in Fig. 11 where the packing structure evolved at a corresponding membrane thickness (in green packing state) can be realized. In

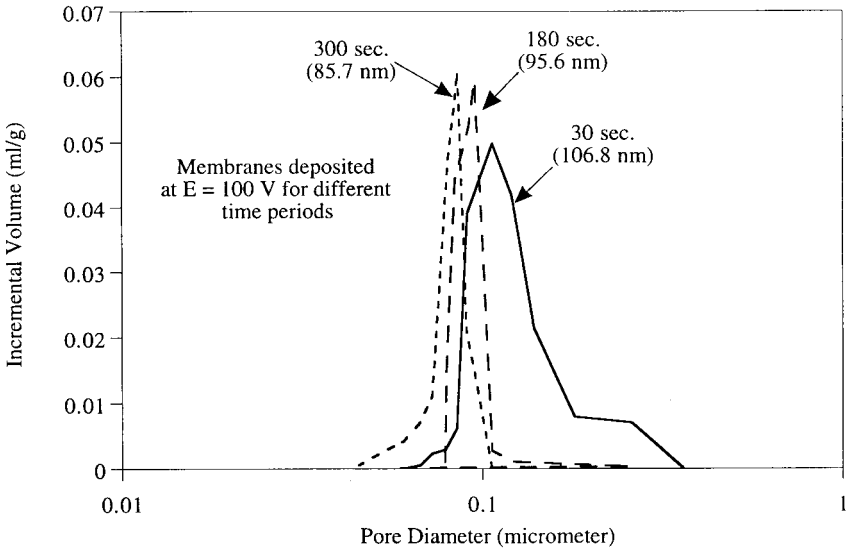

Fig. 10. The pore size distribution of the membranes prepared at $E = 100$ V for various time periods of deposition.

general, below the critical thickness, the solid fraction (or porosity) is generally treated as constant and becomes higher (more dense), with an extent depending on the applied voltage, with increasing thickness. Although two voltages are applied, the trend should be the same for other levels of d.c. voltage as that estimated for $E = 100$ V. For current investigation, it is suggested that the membranes with desirable pore structure, i.e. uniform, small pore size and narrow pore distribution, are likely to be obtained through the use of lower levels of applied voltage for a longer time of deposition.

In fact, the microstructural evolution map depicted in Fig. 11 provided interesting and also more detailed information on layer-by-layer pore structure evolution within a membrane of finite thickness. However, it is sometimes difficult to accurately determine the layer-to-layer change in microstructure and mostly, a bulk packing property (such as porosity, pore size distribution, etc.) of a given membrane can be more easily accessible via experimental measurement (such as mercury porosimetry, BET adsorption, etc.). Therefore, it should be important and interesting to estimate the bulk solid fraction ($f_{\text{bulk}} = 1 - P$) of a given membrane with finite thickness through the use of the microstructural evolution map.

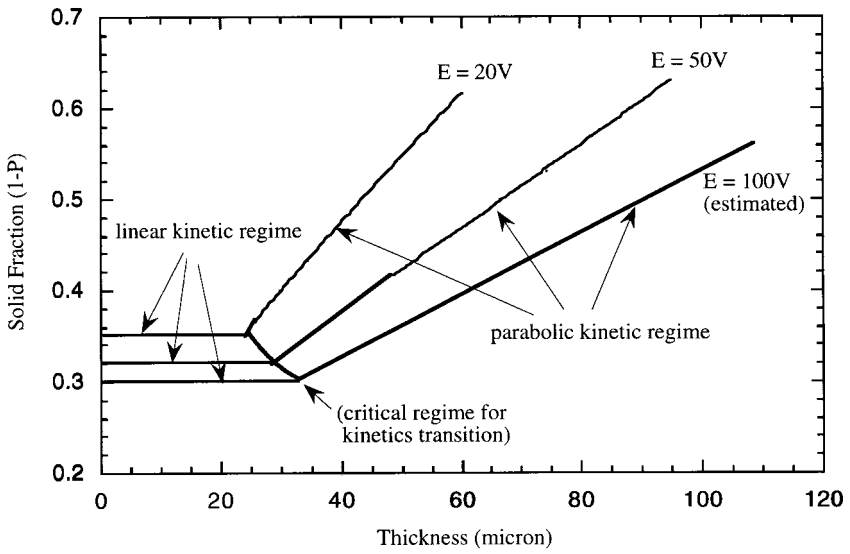

Fig. 11. The microstructural evolution map for the EPD membranes prepared under different voltages, a constant porosity regime over the thickness of 20–30 μm can be obtained.

Table 3. A comparison of porosity value in the EPD membranes between porosimeter measurement and calculation based on equation (13). The membranes were prepared under $E = 100$ V for various deposition times (t)

t (s)	Measured P (volume fraction)	Calculated P (volume fraction)
30	0.797	0.712
180	0.674	0.591
300	0.551	0.513

From the evolution map, the bulk solid fraction of a membrane with a thickness h_m can be treated as a sum of the solid fraction (f_i) of a layer with an infinitesimal thickness (h_i)

$$f_{bulk} = \sum \frac{h_i}{h_m} f_i. \quad (12)$$

After integration and arrangement, equation (12) can be expressed by

$$f_{bulk} = \frac{h_c}{h_m} f_c + \frac{1}{h_m}\left[a(h_m - h_c) + \frac{b}{2}(h_m^2 - h_c^2)\right] \quad (13)$$

where f_c is the solid fraction within the critical thickness previously determined and a and b are constants which can be determined as the intercept and the slope, respectively, of the straight line over the parabolic regime in Fig. 11. Therefore, the first term on the right-hand side of equation (13) represents the solid fraction over the regime dominated by the linear kinetics, whilst the second term, the parabolic kinetics.

To test the feasibility of equation (13), membranes deposited under $E = 100$ V for various time periods were prepared. The porosity of the membranes was then determined using mercury porosimeter, having a thickness (h_m) of 30, 127.7, and 175 μm for the 30, 180, and 300 s of deposition, respectively. The membrane porosity is also calculated using the following values: $a = 0.18$, $b = 0.0034$, $h_c = 33$ μm, and $f_c = 0.29$. The resulting comparison between the measured and the calculated values of the porosity is given in Table 3. The calculated porosity values are generally lower by 6–11% than the measured values. This discrepancy may be due to an overestimate of f_c, originating from the fact that it is difficult to determine the time span for the linear kinetic regime in a precise manner and a longer time span determined by, for instance, visual judging (Fig. 3), would cause a reduction of S_1 values, resulting in a higher value of $(1 - P)$ according to equation (8). However, the porosity prediction from equation (13) can still provide a reasonable estimate for porosity evolution within the real EPD membranes.

4. CONCLUSION

This preliminary study on the fabrication of porous ceramic membranes via an electrophoretic deposition (EPD) technique provides encouraging results. Membranes have been prepared with a controlled pore structure and most interestingly, a porosity gradient along the growing layer. The deposition kinetics of the EPD process was determined in terms of the thickness rather than the weight of deposition. This approach allowed, (which may the first time as far as we know) the pore evolution within the deposited layer to be evaluated via a porosity equation derived from a kinetic model. The deposition kinetics changed from a linear time (t)–thickness (h) function to a parabolic t–h function (i.e. a linear $t^{1/2}$–h function) after some critical time period of deposition. The membranes prepared in the linear t–h regime possessed a less uniform and porous particle packing structure; however, for the parabolic regime, a denser deposited structure was observed both analytically and experimentally as the time of deposition increased.

Acknowledgements—One of the authors (D.M.L.) is gratefully indebted to Minister of Economic Affairs, Taiwan, and the other two (C.Y.C. and S.Y.C.) wish to thank the National Science Council, Taiwan, Republic of China under contract number #NSC 87-2218-E-009-016 for supporting this research work.

REFERENCES

1. Pickard, W. F., *J. electrochem. Soc.*, 1968, **115**, 105C.
2. Shimbo, M., Tanzawa, K., Migakawa, M. and Emoto, T., *J. electrochem. Soc.*, 1985, **132**, 393.
3. Brown, D. R. and Salt, F. W., *J. appl. Chem.*, 1963, **15**, 40.
4. Okamura, P. S., Tsukamoto, T. and Koura, N., *Japan J. appl. Phys.*, 1993, **32**, 4182.
5. Nishimori, H., Tasumisago, M. and Minami, T., *J. Ceram. Soc. Japan Int. Ed.*, 1995, **103**, 78.
6. Nagai, M., Yamashita, K., Umegaki, T. and Takuma, Y., *J. Am. Ceram. Soc.*, 1993, **76**(1), 253.
7. Sarkar, P., Haung, X. and Nicholson, P. S., *J. Am. Ceram. Soc.*, 1992, **75**(10), 2907.
8. Fisher, R., Fisher, E., De Portu, G. and Ronear, E., *J. Mater. Sci. Lett.*, 1995, **14**, 25.
9. Julbe, A., Guizard, C., Larbat, A., Cot, L. and Giroir-Fendler, A., *J. Membrane Sci.*, 1993, **77**, 137.
10. Ulhorn, R. J. R., Keizer, K. and Burggraaf, A. J., *J. Membrane Sci.*, 1992, **66**, 271.
11. Kerkar, A. V., U.S. Patent No. 5,340,779.
12. Friedman, S. D., Kerkar, A. V., Hughes, E. W., Brezny, R., Lau, J. W. and Block, J., U.S. Patent No. 5,591,691.
13. Wang, G., Sarkar, P. and Nicholson, P. S., *J. Am. Ceram. Soc.*, 1997, **80**(4), 965.
14. Zhang, Z., Huang, Y. and Jiang, E., *J. Am. Ceram. Soc.*, 1994, **77**(7), 1946.
15. Hirata, Y., Nishimoto, A. and Ishihara, Y., *Nippon Seramikkus Kyokai Gakujutusu Ronbunshi*, 1991, **99**(2), 108.
16. Sussman, A. and Ward, T. J., *RCA Rev.*, 1985, **42**, 178.
17. Leenaar, A. F. M., Keizer, K. and Burggraaf, A. J., *J. Membrane Sci.*, 1985, **19**, 1077.
18. Leenaar, A. F. M. and Burggraaf, A. J., *J. Colloid Interface Sci.*, 1985, **105**(1), 27.
19. Larbot, A., Fabre, J. P., Guizard, C., Cot, L. and Gillot, G., *J. Am. Ceram. Soc.*, 1989, **72**(2), 257.